[1] C. Nitschke, S. M. O'Flaherty, M. Kröll, W. J. Blau, *J. Phys. Chem. B* **2004**, *108*, 1287.
[2] F. E. Hernández, S. Yang, E. W. Van Stryland, D. J. Hagan, *Opt. Lett.* **2000**, *25*, 1180.
[3] N. M. B. Neto, C. R. Mendonca, L. Misoguti, S. C. Zilio, *Opt. Lett.* **2003**, *28*, 191.
[4] N. Izard, C. Ménard, D. Riehl, E. Doris, C. Mioskowski, E. Anglart, *Chem. Phys. Lett.* **2004**, *391*, 124.
[5] X. Sun, R. Q. Yu, G. Q. Xu, T. S. A. Hor, W. Ji, *Appl. Phys. Lett.* **1998**, *73*, 3632.
[6] L. Vivien, P. Lancon, D. Riehl, F. Hache, E. Anglaret, *Carbon* **2002**, *40*, 1789.
[7] L. Vivien, D. Riehl, F. Hache, E. Anglaret, *Physica B (Amsterdam, Neth.)* **2002**, *323*, 233.
[8] X. Sun, Y. Xiong, P. Chen, J. Lin, W. Ji, J. H. Lim, S. S. Yang, D. J. Hagan, E. W. Van Stryland, *Appl. Opt.* **2000**, *39*, 1998.
[9] L. Vivien, D. Riehl, F. Hache, E. Anglaret, *J. Nonlinear Opt. Phys. Mater.* **2000**, *9*, 297.
[10] L. Vivien, D. Riehl, P. Lancon, F. Hache, E. Anglaret, *Opt. Lett.* **2001**, *26*, 223.
[11] L. Vivien, D. Riehl, J. F. Delouis, J. A. Delaire, F. Hache, E. Anglaret, *J. Opt. Soc. Am. B* **2002**, *19*, 208.
[12] P. Chen, X. Wu, X. Sun, J. Lin, W. Ji, K. L. Tan, *Phys. Rev. Lett.* **1999**, *82*, 2548.
[13] Y. H. Meyer, M. Pittman, P. Plaza, *J. Photochem. Photobiol., A* **1998**, *114*, 1.
[14] T. Xia, D. J. Hagan, A. Dogariu, A. A. Said, E. W. Van Stryland, *Appl. Opt.* **1997**, *36*, 4110.
[15] M. Pittman, P. Plaza, M. M. Martin, Y. H. Meyer, *Opt. Commun.* **1998**, *158*, 201.
[16] J. H. Lim, O. V. Przhonska, S. Khodja, S. Yang, T. S. Ross, D. J. Hagan, E. W. Van Stryland, M. V. Bondar, Y. L. Slominsky, *Chem. Phys.* **1999**, *245*, 79.
[17] R. S. Lepkowicz, O. V. Przhonska, J. M. Hales, J. Fu, D. J. Hagan, E. W. Van Stryland, M. V. Bondar, Y. L. Slominsky, A. D. Kachkovski, *Chem. Phys.* **2004**, *305*, 259.
[18] X. R. Zhu, J. M. Harris, *Chem. Phys.* **1990**, *142*, 301.
[19] S. N. R. Swatton, K. R. Welford, S. J. Till, *Appl. Phys. Lett.* **1995**, *66*, 1868.
[20] I. Martini, G. V. Hartland, *Chem. Phys. Lett.* **1996**, *258*, 180.
[21] R. Lepkowicz, A. Kobyakov, D. J. Hagan, E. W. Van Stryland, *J. Opt. Soc. Am. B* **2002**, *19*, 94.
[22] S. Hughes, G. Spruce, B. S. Wherrett, K. R. Welford, A. D. Lloyd, *Opt. Commun.* **1993**, *100*, 113.
[23] S. Hughes, B. Wherrett, *Phys. Rev. A: At., Mol., Opt. Phys.* **1996**, *54*, 3546.
[24] X. Deng, X. Zhang, Y. Wang, Y. Song, S. Liu, C. Li, *Opt. Commun.* **1999**, *168*, 207.
[25] K. Jiang, A. Eitan, L. S. Schadler, P. M. Ajayan, R. W. Siegel, N. Grobert, M. Mayne, M. Reyes-Reyes, H. Terrones, M. Terrones, *Nano Lett.* **2003**, *3*, 275.
[26] M. Reyes-Reyes, N. Grobert, R. Kamalakaran, T. Seeger, D. Golberg, M. Rühle, Y. Bando, H. Terrrones, M. Terrones, *Chem. Phys. Lett.* **2004**, *396*, 167.
[27] M. Mayne, N. Grobert, M. Terrones, R. Kamalakaran, M. Rühle, H. W. Kroto, D. R. M. Walton, *Chem. Phys. Lett.* **2001**, *338*, 101.

Fabrication of Three-Dimensional Surface Structures with Highly Fluorescent Quantum Dots by Surface-Templated Layer-by-Layer Assembly**

By *Dejian Zhou*, *Andreas Bruckbauer*, *Chris Abell*, *David Klenerman*,* and *Dae-Joon Kang**

Highly fluorescent quantum dots (QDs) are currently of great interest due to their unique size-dependent properties,[1] and have many applications in ultrahigh-sensitivity bioimaging,[2] photonic and optoelectronic devices, and electroluminescent light-emitting diodes (LEDs).[3] Their sizes, typically on the order of a few nanometers, make them excellent building blocks for nanoscience and for fabrication of hybrid structures. QDs have recently been incorporated into fluorescent thin films through layer-by-layer (LbL) assembly[4] of charged QDs with oppositely charged polymers.[5–7] These studies were mostly carried out on flat surfaces and did not result in patterned structures. However, to integrate these films into possible photonic or optoelectronic devices, it is necessary to control the location of the fabricated structures on a surface.

Fluorescent patterns made of QDs and/or nanoparticles have recently been prepared. These patterns were fabricated by photolithography or electron-beam patterning in combination with the "lift-off" technique,[8,9] by microcontact printing (μCP) of QD–dendrimer nanocomposites,[10] by selective dewetting on organic templates,[11] by capillary organization,[12] and by photoactivation of low-quantum-efficiency QDs.[13] Most of the patterns fabricated to date contain just a single QD layer, with fluorescence signal-to-background ratios typically smaller than 100. This may limit their application in devices where multiple-layered structures and/or a higher signal-to-background ratio are required, for example, in a recently reported exciton-recycling structure.[6]

LbL assembly is a powerful and versatile approach for the fabrication of multilayer films of charged materials.[4,5] However, its selectivity for patterning QDs is often limited by

[*] Dr. D.-J. Kang, Dr. D. Zhou
Nanoscience Centre, University of Cambridge
11 J. J. Thomson Avenue, Cambridge CB3 0FF (UK)
E-mail: djk1003@cam.ac.uk
Dr. D.-J. Kang
Sungkyunkwan Advanced Institute of Nanotechnology, and
Department of Physics, Sungkyunkwan University
Suwon, 440-746 (Korea)
Dr. D. Klenerman, Dr. A. Bruckbauer, Prof. C. Abell
Department of Chemistry, University of Cambridge
Lensfield Road, Cambridge CB2 1EW (UK)
E-mail: dk10012@cam.ac.uk

[**] This work was supported by the Cambridge Interdisciplinary Research Collaboration (IRC) in Nanotechnology (UK). Supporting Information is available online from Wiley InterScience or from the author.

 DOI: 10.1002/adma.200401520

ADVANCED MATERIALS

strong and indiscriminate secondary interactions.[13] By LbL-coating the QD surfaces with charged polymers, fluorescent micropatterns consisting of a bilayer of QDs with two different colors have recently been prepared by Belcher and coworkers.[14] It was not clear whether the selectivity could be maintained over multiple bilayers. We have found, and report here, that the selectivity on patterned surfaces shown in the first few layers can decrease dramatically and almost disappear after tens of bilayers are assembled. Thus, improving the selectivity on the patterned features while reducing the non-specific adsorption on the resist region are key to producing devices where multiple layers of QDs are required.[6] This is an important issue in LbL assembly. In this communication, we show that by reducing the non-specific interactions through the modification of QD surface coatings and by employing a polymer with a hydrophilic backbone, it is possible to achieve high levels of selectivity in the LbL assembly of QDs up to at least 20 bilayers.

Our method is based on patterning of a gold surface with self-assembled monolayers (SAMs) of alkyl thiols with tailored surface properties.[15] A SAM of an alkyl thiol terminated with a hexa(ethylene glycol) group, known to be effective in resisting non-specific adsorption of biomolecules and nanoparticles,[16] was used as the resistive coating. To promote the adsorption of the charged QDs, a SAM terminated with either a pyridinium or a carboxylic acid (COOH) group[17] was used. The gold surface was patterned on the microscale by μCP,[18] and then the unstamped regions were functionalized with a second SAM by solution self-assembly. To reduce the possibility of thiol exchange during incubation, a thiol with a longer alkyl chain, which forms a more stable SAM,[15] was used to stamp, and a thiol with a shorter chain was used for backfilling. For example, when using 16-mercaptohexadecanoic acid (MHDA, C_{15}) and 11-mercaptoundecylhexa(ethylene glycol) alcohol (EG_6OH, C_{11}), MHDA was used to stamp, but when EG_6OH and 6-mercaptohexyl-*N*-pyridinium bromide (MHPBr, C_6) were used, EG_6OH was used to stamp. μCP was employed for surface patterning due to its experimental simplicity. Furthermore, it is a parallel method capable of producing micro- to nanoscale surface patterns over a centimeter-scale area in minutes, without the need of expensive equipment and/or a clean-room environment.[18] A glass coverslip coated with a thin layer of gold (~40 % transmission, typical roughness less than 1 nm over 25 μm^2)[16b] or a freshly prepared template-stripped gold (TSG) surface (typical roughness less than 0.3 nm over 25 μm^2)[19] was used as the substrate. After μCP patterning followed by backfilling, the patterned surfaces were subsequently used to template the LbL growth of the QD and polymer.

At first, a commercial water-soluble CdSe/ZnS core–shell Evidot (COOH-QD) with a surface coating terminated with COOH groups was used. The QDs were negatively charged under the assembly conditions in phosphate buffer (10 mM phosphate, 1 mM NaN_3, pH 7.5) due to deprotonation of surface COOH groups. The QDs were readily adsorbed onto an oppositely charged surface by electrostatic attraction. The size of the QDs was verified by atomic force microscopy (AFM). Incubation of an MHP SAM-coated TSG surface with the QD solution (0.025 mg mL^{-1} in phosphate buffer, pH 7.5) for 30 min resulted in adsorption of the QDs onto the surface. The AFM topographic image (Supporting Information, Fig. S1a) shows that the QDs were randomly adsorbed on the substrate surface, with the majority of the QDs being isolated and only a few clumped together to form taller domains. A simultaneously recorded phase image (Fig. S1b) confirms that these higher domains are due to aggregation of the QDs. The QDs still maintained their structural identity within the aggregates, as suggested by the existence of clear gaps among the QDs in the phase image. The height histogram shows that the majority of the diameters of the QDs was within a narrow distribution around 4.7 nm. The measured heights (diameters) of the QDs (~4.7 nm) were in good agreement with the size of the QDs (nominal crystal diameter 4.1 nm), taking into account the thickness of the surface coating.

Next, the LbL assembly of the COOH-QDs on patterned surfaces was investigated. Poly(allylamine) (PA), a positively charged polymer widely used in LbL assembly,[20] was used as the assembly partner. A glass coverslip, coated with a thin layer of gold and patterned with 2 μm SAM stripes of MHP (for specific attachment of the QDs) separated by 2 μm SAM stripes of EG_6OH (to resist non-specific adsorption), was used. Incubation of the patterned thin-gold-layer surface with the COOH-QD solution resulted in selective adsorption of the QDs onto the MHP stripes (Fig. 1a). The fluorescence intensity was relatively weak, with a signal-to-background ratio (fluorescence intensity ratio between the MHP and the EG_6OH stripes) of only ~5. The value is comparable to that of previously reported photogenerated protein patterns.[21] The low signal-to-background ratio is possibly due to quenching of the QD fluorescence by the gold layer underneath since the separation is only ~2 nm (the MHP SAM was ~1.6 nm thick[17] and the QD surface coating was ~0.3 nm thick). In addition, the QDs were found to have only covered a fraction of the MHP surface (Fig. S1a). After a further treatment of this surface with PA followed by COOH-QD (an assembly cycle, abbreviated as (PA/QD)), the signal-to-background ratio was significantly improved to ~55. The fluorescence intensity on the MHP region increased significantly, while the background remained almost constant (Fig. 1b). This was presumably due to the second-layer QD being further separated from the gold surface, so the quenching by the gold was greatly reduced. Another possibility could be that more QDs were assembled on the PA surface than the first layer on the flat MHP surface due to increased surface roughness (and therefore, increased surface area).

As the LbL assembly progressed, QDs were also found to adsorb onto the EG_6OH resist region (Fig. 1c) and as a result, the signal-to-background ratio decreased significantly. A plot of the average fluorescence intensity versus the number of assembly cycles (Fig. 2a) reveals that the fluorescence intensity of the MHP region increased linearly with the number of as-

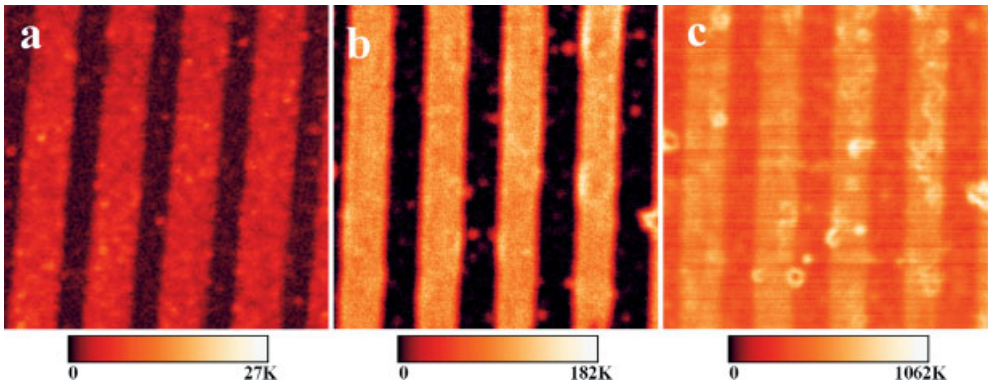

Figure 1. Fluorescence images following the LbL assembly process of COOH-QD and PA on μCP-patterned 2 μm SAM stripes of MHP within an EG_6OH SAM background on a thin-gold-layer-coated glass coverslip under 0.5 μW laser excitation (488 nm). Film structures assembled on top of the SAM template are a) QD, b) (QD/PA)/QD, and c) $(QD/PA)_4$/QD. Image sizes: 19 μm × 19 μm. The fluorescence scale bars are depicted beneath each image.

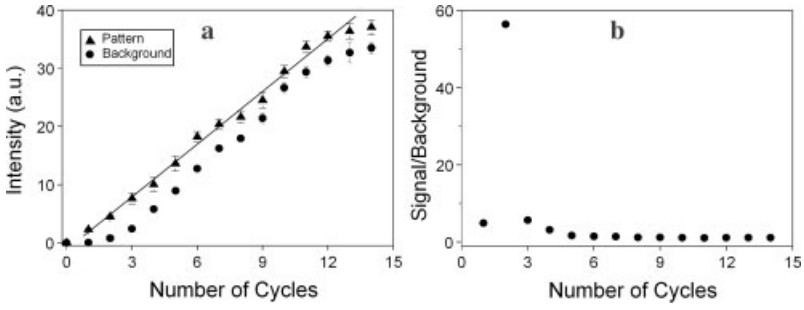

Figure 2. a) Plot of the average fluorescence intensity versus the number of QD/PA assembly cycles on the MHP pattern (▲) and the EG_6OH resist (●). b) Plot of the fluorescence signal-to-background ratio (ratio of fluorescence intensity of the MHP pattern to the EG_6OH resist background) versus the number of assembly cycles.

sembly cycles, suggesting linear growth of the COOH-QD/PA films. On the EG_6OH resist region, the fluorescence exhibited a slow growth for the first three cycles, after which the intensity also increased linearly with the number of cycles. This suggests that the EG_6OH was only effective at resisting the build-up of the QD/PA films during the early cycles. This is presumably due to the presence of non-specific adsorptions of the QDs and PA onto the EG_6OH surface, possibly starting at gold domain boundaries and/or surface defects. The non-specific adsorption gradually spread and covered more and more of the EG_6OH resist surface as the LbL assembly proceeded and finally reached full coverage, completely changing the surface properties. After this point, the growth rate became linear and similar to that as on the MHP surface. As a result, the difference in fluorescence intensity between the two surface regions remained almost constant. A plot of the fluorescence signal-to-background ratio (an indication of the selectivity for the LbL assembly on the two surfaces) versus the number of assembly cycles (Fig. 2b) reveals that after an initial increase from the first (QD) to the second cycle (QD/PA/QD), the signal-to-background ratio gradually but significantly decreased as more and more layers were assembled.

The adsorption on the EG_6OH resist surface was thought to be mainly due to non-specific interactions, such as hydrophobic interactions and hydrogen bonding. To reduce hydrogen bonding between the QDs and the EG_6OH surface, another red QD with a surface coating terminated with negatively charged sulfonate groups was prepared. This was obtained by treatment of a hydrophobic trioctylphosphine oxide (TOPO)-capped CdSe/ZnS Evidot (color: Fort Orange) with 2-mercaptoethanesulfonic acid (MESA) sodium salt.[22] This treatment led to ligand exchange on the QD surface coating, forming water-soluble MESA-capped QDs (MESA-QDs). In addition, linear poly(ethyleneimine) (LPEI), a positively charged polymer with a hydrophilic backbone, was selected as the assembly partner.[23] This should reduce the undesirable hydrophobic interactions and hydrogen bonding with the EG_6OH resist surface.

As expected, the LbL assembly of the LPEI/MESA-QD did indeed exhibit a high level of selectivity on a μCP-patterned MHDA SAM dot array within the EG_6OH resist background. The assembly, initiated by a first treatment of the surface with the LPEI solution, followed by MESA-QD (abbreviated as (LPEI/MESA-QD)), yielded selective build-up of the polymer/QD composite on the patterned features alone. Representative fluorescence images after 2 and 19 cycles are shown in Figures 3a,b, respectively. It is clear that the assembly took place almost exclusively on the MHDA patterns, with little non-specific adsorption on the EG_6OH resist background even after 20 cycles (except at regions of surface imperfections caused by μCP). This was further confirmed by the AFM topographic image (Fig. 3d) collected on the same sample after 20 cycles. The averaged line-scan profile revealed that the patterns were ~85 nm high. This corresponds to a thickness of ~4.1 nm per (LPEI/MESA-QD) bilayer, assuming a uniform and linear growth of the polymer–QD layers.[24]

ADVANCED MATERIALS

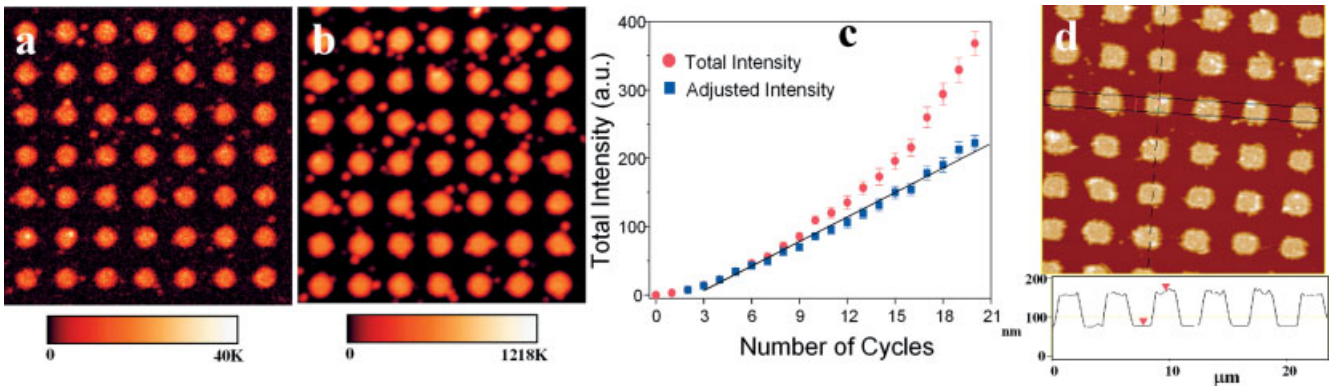

Figure 3. Fluorescence images showing the LbL assembly of MESA-QD with LPEI on μCP-patterned MHDA surface arrays within EG_6OH resist background; images shown are for a) 2 and b) 19 cycles. Image size: 30 μm × 30 μm. c) Plot of the total fluorescence intensity (red dots) and the area-normalized fluorescence intensity (blue squares) versus the number of assembly cycles. d) AFM topographic images of the $(LPEI/QD)_{20}$ assembled on the patterned thin-gold-layer surface.

The plot of the average pixel fluorescence intensity[25] over the whole image versus the number of assembly cycles shows that the fluorescence increased nonlinearly with the number of cycles (Fig. 3c, solid red circles, and Fig. S2A). However, comparing the two fluorescence images shown in Figures 3a,b, it is evident that not only did the fluorescence intensity increase with the number of assembly cycles, but the feature sizes also increased. The patterned features grew both vertically and horizontally. An analysis of the fluorescence images shows that the total fluorescence area within the image area increased roughly linearly with the number of assembly cycles (Fig. S2B). The area-normalized fluorescence intensity (fluorescence intensity divided by fluorescence area) exhibited a linear growth with the number of cycles from the third cycle onwards (Fig. 3c, solid blue squares). The weaker fluorescence growth for the first three cycles may be caused by fluorescence quenching by the gold and the influence of the initial surface coating, which has been demonstrated to strongly affect the LbL growth of charged polymers.[26] The averaged fluorescence intensity from the central part of the features also exhibited a linear increase with the number of cycles after the first four cycles (Fig. S2C). All these observations suggest that although the fluorescence intensity (the number of QDs) grew nonlinearly with the number of cycles due to horizontal growth of the features, the vertical growth was actually linear.

The horizontal growth of the features may be caused by the shape of the LPEI, which is thread-like and up to ~200 nm long when fully extended (for a polymer of average molecular weight 25 000 g mol^{-1}). When adsorbed onto an oppositely charged pattern, it is probable that not all the polymer chains were completely coiled and protruded above the features. Some polymers may hang over the EG_6OH resist surface. This part of the polymer chain could serve as the base for future LbL growth of the QDs and polymers. This idea is supported by the observation that some of the features had smaller interconnected features, as seen in both fluorescence and AFM topographic images.

It should be noted that the MESA-QD/LPEI exhibited a far higher level of selectivity towards the pattern over the resist background than the COOH-QD/PA combination. The fluorescence signal-to-background ratio (excluding the surface-imperfection regions caused by μCP) increased dramatically as the LbL process progressed (Fig. 4), reaching ~7000 after 16 cycles. This signal-to-background ratio is two orders of magnitude higher than previously obtained fluorescence

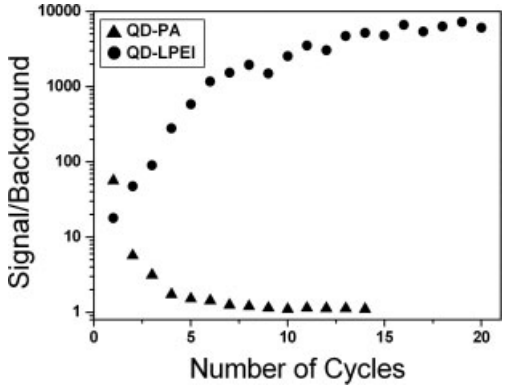

Figure 4. Plot of the fluorescence signal-to-background ratio for the COOH-QD/PA (▲) and the MESA-QD/LPEI (●) versus the number of assembly cycles.

patterns,[21] demonstrating the excellent selectivity in this combination. In contrast, the signal-to-background ratio for the COOH-QD/PA combination decreased dramatically as more layers were assembled (~1.2 after 10 cycles). This was presumably because LPEI is a linear hydrophilic polymer with no side chains. Under our experimental conditions, LPEI (and the QDs) are both highly hydrated and would be repelled from the hydrated EG_6OH SAM resist surface, resulting in little adsorption. Thus, the signal-to-background ratio improves as the LbL assembly proceeds, since QDs build up

on the features alone. On the other hand, PA is composed of positively charged amine side chains and a hydrophobic alkyl backbone. It can non-specifically adsorb onto the EG_6 resist through hydrophobic interactions and hydrogen bonding between its side-chain amines and the oxygen atoms in the hexa(ethylene glycol) chains of the EG_6OH resist. The non-specific adsorption on the background region gradually becomes more significant as the LbL assembly proceeds, resulting in a reduced signal-to-background ratio.

Finally, we show it is possible to fabricate three-dimensional (3D) structures with QD_1–QD_2 combinations.[14] For this, the commercially available COOH-QD (red) and a green QD with an amine-terminal coating (NH_2-QD) were used. LbL assembly of the NH_2-QD and the COOH-QD on a patterned MHDA dot array within an EG_6OH background led to selective build-up of 3D structures. Fluorescence images obtained from the green and red channels (Figs. 5a,b) clearly demonstrated the selective build-up of the green-QD/red-QD assemblies. The AFM topographic image taken after 7.5 cycles ($(NH_2\text{-QD/COOH-QD})_7(NH_2\text{-QD})$) (Fig. 5c) confirmed that the QDs assembled on the MHDA patterns alone, with little evidence of non-specific adsorption on the EG_6OH background region. The average height of the features, as shown in the averaged line-scan profiles, was ~50 nm. It was also possible to extend this assembly to produce hierarchical 3D structures, such as the $(\text{QD/polymer})_n(\text{QD/QD})_m$ combination (Fig. S3), simply by changing the assembly partners during the LbL-assembly process.

In summary, we have demonstrated that by modification of the QD surface coatings, choosing proper assembly partners, and using a surface-resist coating to reduce the non-specific secondary interactions, it is possible to selectively build up 3D surface structures with highly fluorescent QDs. The signal-to-background ratio obtained of ~7000 is two orders of magnitude greater than those reported in earlier studies, demonstrating the excellent selectivity in our multilayer assembly. The height of the features could be controlled easily by variation of the number of assembly cycles. In principle, the assembly can be miniaturized to the nanometer scale, and the components of the assembly could be tailored to accommodate different materials to introduce different functionalities, making this process an easy and versatile means of fabrication of highly hierarchical nanoscale 3D assemblies and/or devices with QDs over macroscopic surface areas.

Experimental

Materials: 11-Mercaptoundecylhexa(ethylene glycol) alcohol (EG_6OH) and 6-mercaptohexyl-*N*-pyridinium bromide (MHPBr) were synthesized as described elsewhere [16b,17]. 16-Mercaptohexadecanoic acid (MHDA, 90 %), mercaptoethanesulfonic acid (MESA, sodium salt, 98 %), poly(allylamine) (PA, molecular weight [MW] 65 000 g mol^{-1}), and other reagents were purchased from Sigma–Aldrich (Dorset, UK). MHDA was purified as described previously [17]. Linear poly(ethyleneimine) (LPEI, MW 25 000 g mol^{-1}) was purchased from Polysciences Inc. (Warrington, PA). Aqueous solutions of carboxylic-acid-capped CdSe/ZnS core–shell quantum dots (QDs) (COOH-QD, Fort Orange, first exciton peak at 586 nm) and amine-capped CdSe/ZnS core–shell QDs (NH_2-QD, Adirondack Green, first exciton peak at 505 nm), and a toluene solution of trioctylphosphine oxide (TOPO)-capped CdSe/ZnS core–shell QDs (TOPO-QD, Fort Orange, first exciton peak at 586 nm) were purchased from Evident Technologies (Troy, NY). The TOPO-QDs were rendered water-soluble by ligand exchange with MESA following a literature procedure (~20 % of the treated QDs were water-soluble) [22]. After ligand exchange, the MESA-capped QDs were dissolved and diluted in phosphate buffer (10 mM phosphate, 1 mM NaN_3, pH 7.5). All solutions were filtered with a Whatman syringe filter (0.02 μm pore size) before use. Glass coverslips coated with a thin layer of gold (~5 nm thick gold layer with a Ti adhesion layer, roughness <1 nm over 25 μm^2) were obtained from Ssens BV (Hengelo, The Netherlands) [16b]. Template-stripped gold (TSG) surfaces were prepared as described previously [19]. Freshly stripped TSG surfaces were used to minimize contamination [27].

Microcontact Printing (μCP): Two poly(dimethylsiloxane) (PDMS) stamps, one with features of 2 μm square arrays and the other with 2 μm stripes, were used. The stamp was inked with a 2 mM solution of MHDA (in 2-butanol) or EG_6OH (in ethanol) with a cotton swab. After being dried with N_2, the stamp was brought into conformal

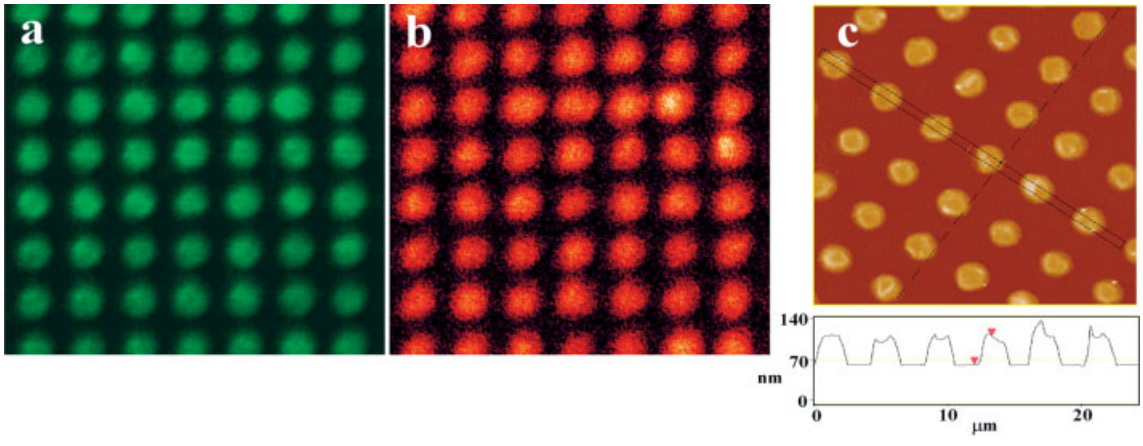

Figure 5. Fluorescence images of $(NH_2\text{-QD/COOH-QD})_7/NH_2\text{-QD}$ assembled on the μCP-patterned MHDA patterns within the EG_6OH background on a thin-gold-layer-coated glass coverslip under 0.5 μW laser excitation at 488 nm. a) Green channel, b) red channel. Image size: 30 μm × 30 μm. c) Tapping-mode AFM topographic image of the same surface shown in (a,b). Image size: 20 μm × 20 μm.

ADVANCED MATERIALS

contact with a thin-gold-layer-coated glass coverslip for 20–30 s. The unstamped surfaces were then filled with a self-assembled monolayer (SAM) of the EG_6OH (for MHDA) or MHPBr (for EG_6OH) by incubation of the surface with a 1 mM solution of EG_6OH (in ethanol) or MHPBr (in water) for 1 h, rinsing with ethanol and water, and drying with N_2 [18].

Layer-by-Layer (LbL) Assembly: All the LbL assemblies were carried out in phosphate buffer (10 mM phosphate, 1 mM NaN_3, pH 7.5). Concentrations of 0.025 mg mL^{-1} for the QDs and 1 mg mL^{-1} for the polymers were used. The μCP-patterned surface was incubated with a polymer solution for 15 min and rinsed with the buffer, then incubated with a QD solution for 30 min, followed by a rinse with buffer (this constitutes an assembly cycle of (polymer/QD)). The process was repeated until a desired number (n) of bilayers ($(polymer/QD)_n$) were deposited. The same procedure was used in the QD–QD assembly, and 30 min incubation times were used for both QDs.

Atomic Force Microscopy (AFM): All AFM images were collected in tapping mode on a Digital Instrument (Veeco, CA) Dimension 3100 AFM with a Nanoscope IV controller in air at 24 ± 1 °C. Ultrasharp MikroMasch silicon cantilevers (125 μm long, tip radius < 10 nm, spring constant ~40 N m^{-1}, resonant frequency 330 kHz) were used. Topographic and phase images were simultaneously collected at 512 × 512 pixels per image at 0.8 to 1 Hz. The captured images were analyzed with the Nanoscope image-analysis software using first-order flattening [16b,27].

Fluorescence Imaging: Fluorescence images were recorded under 0.5 μW laser excitation at 488 nm on a home-built scanning confocal microscope (SCM) [28]. Details of the setup are given in the Supporting Information. The integration time was 1 ms per pixel, and images were collected at 256 × 256 or 512 × 512 pixels per image. Images were processed using WSxM 3.0 (Nanotec Electronica S.L., Spain). The averaged fluorescence intensity was obtained by converting the image into grayscale and then analyzing using the histogram function in Adobe Photoshop (Version 6.0).

Received: September 16, 2004
Final version: January 11, 2005
Published online: April 4, 2005

[1] A. P. Alivisatos, *Science* **1996**, *271*, 933.
[2] W. C. W. Chan, S. M. Nie, *Science* **1998**, *281*, 2016.
[3] a) V. L. Colvin, M. C. Schlamp, A. P. Alivisatos, *Nature* **1994**, *370*, 354. b) W. U. Huynh, J. J. Dittmer, A. P. Alivisatos, *Science* **2002**, *295*, 2425.
[4] a) G. Decher, *Science* **1997**, *277*, 1232. b) P. T. Hammond, *Curr. Opin. Colloid Interface Sci.* **1999**, *4*, 430. c) C. F. J. Faul, M. Antonietti, *Adv. Mater.* **2003**, *15*, 673.
[5] a) A. L. Rogach, D. S. Koktysh, M. Harrison, N. A. Kotov, *Chem. Mater.* **2000**, *12*, 1526. b) A. A. Mamedov, A. Belov, M. Giersig, N. N. Mamedova, N. A. Kotov, *J. Am. Chem. Soc.* **2001**, *123*, 7738. c) M. T. Crisp, N. A. Kotov, *Nano Lett.* **2003**, *3*, 173. d) N. A. Kotov, I. Dekany, J. H. Fendler, *J. Phys. Chem.* **1995**, *99*, 13 065.
[6] T. Franzl, T. A. Klar, S. Schietinger, A. L. Rogach, J. Feldmann, *Nano Lett.* **2004**, *4*, 1599.
[7] L. I. Halaoui, *Langmuir* **2001**, *17*, 7130.
[8] a) F. Hua, T. H. Cui, Y. Lvov, *Langmuir* **2002**, *18*, 6712. b) F. Hua, J. Shi, Y. Lvov, T. Cui, *Nano Lett.* **2002**, *2*, 1219.
[9] a) M. H. V. Werts, M. Lambert, J. P. Bourgoin, M. Brust, *Nano Lett.* **2002**, *2*, 43. b) J. Won, K. J. Ihn, Y. S. Kang, *Langmuir* **2002**, *18*, 8246.
[10] W. C. Wu, A. M. Bittner, K. Kern, *Adv. Mater.* **2004**, *16*, 413.
[11] N. Lu, X. D. Chen, D. Molenda, A. Naber, H. Fuchs, D. V. Talapin, H. Weller, J. Muller, J. M. Lupton, J. Feldmann, A. L. Rogach, L. F. Chi, *Nano Lett.* **2004**, *4*, 885.
[12] Y. Cui, M. T. Bjork, J. A. Liddle, C. Sonnichsen, B. Boussert, A. P. Alivisatos, *Nano Lett.* **2004**, *4*, 1093.
[13] Y. Wang, Z. Y. Tang, M. A. Correa-Duarte, L. M. Liz-Marzan, N. A. Kotov, *J. Am. Chem. Soc.* **2003**, *125*, 2830.
[14] S. Jaffar, K. T. Nam, A. Khademhosseini, J. Xing, R. S. Langer, A. M. Belcher, *Nano Lett.* **2004**, *4*, 1421.
[15] a) M. D. Porter, T. B. Bright, D. L. Allara, C. E. D. Chidsey, *J. Am. Chem. Soc.* **1987**, *109*, 3559. b) C. D. Bain, J. Evall, G. M. Whitesides, *J. Am. Chem. Soc.* **1989**, *111*, 7155.
[16] a) K. L. Prime, G. M. Whitesides, *J. Am. Chem. Soc.* **1993**, *115*, 10 714. b) D. Zhou, A. Bruckbauer, L. M. Ying, C. Abell, D. Klenerman, *Nano Lett.* **2003**, *3*, 1517. c) B. Kannan, R. P. Kulkami, A. Majumdar, *Nano Lett.* **2004**, *4*, 1521.
[17] D. J. Zhou, X. Z. Wang, L. Birch, T. Rayment, C. Abell, *Langmuir* **2003**, *19*, 10 557.
[18] a) Y. N. Xia, J. A. Rogers, K. E. Paul, G. M. Whitesides, *Chem. Rev.* **1999**, *99*, 1823. b) B. Michel, A. Bernard, A. Bietsch, E. Delamarche, M. Geissler, D. Juncker, H. Kind, J. P. Renault, H. Rothuizen, H. Schmid, P. Schmidt-Winkel, R. Stutz, H. Wolf, *IBM J. Res. Dev.* **2001**, *45*, 697.
[19] a) P. Wagner, M. Hegner, H. J. Guntherodt, G. Semenza, *Langmuir* **1995**, *11*, 3867. b) D. J. Zhou, K. Sinniah, C. Abell, T. Rayment, *Langmuir* **2002**, *18*, 8278.
[20] X. P. Jiang, S. L. Clark, P. T. Hammond, *Adv. Mater.* **2001**, *13*, 1669.
[21] J. Doh, D. J. Irvine, *J. Am. Chem. Soc.* **2004**, *126*, 9170.
[22] a) H. Mattoussi, J. M. Mauro, E. R. Goldman, G. P. Anderson, V. C. Sundar, F. V. Mikulec, M. G. Bawendi, *J. Am. Chem. Soc.* **2000**, *122*, 12 142. b) S. F. Wuister, I. Swart, F. van Driel, S. G. Hickey, C. D. Donega, *Nano Lett.* **2003**, *3*, 503.
[23] S. L. Clark, E. S. Handy, M. F. Rubner, P. T. Hammond, *Adv. Mater.* **1999**, *11*, 1031.
[24] The features appear to be circular in the fluorescence image, but they are square-like in the AFM image. This may be due to the resolution difference of the two techniques. Scanning confocal microscopy has a lower resolution (~300 nm, in the case of our equipment), thus the fluorescence image may not represent the real shape of the features.
[25] The fluorescence was always monitored from the same region on the surface, so the average pixel intensity should be proportional to the number of QDs present in the image if there is no quenching.
[26] D. J. Zhou, A. Bruckbauer, M. Batcholar, D.-J. Kang, C. Abell, D. Klenerman, *Langmuir* **2004**, *20*, 9089.
[27] D. J. Zhou, K. Sinniah, C. Abell, T. Rayment, *Angew. Chem. Int. Ed.* **2003**, *42*, 4934.
[28] a) A. Bruckbauer, D. J. Zhou, L. M. Ying, Y. E. Korchev, C. Abell, D. Klenerman, *J. Am. Chem. Soc.* **2003**, *125*, 9834. b) A. Bruckbauer, D. J. Zhou, D. J. Kang, Y. E. Korchev, C. Abell, D. Klenerman, *J. Am. Chem. Soc.* **2004**, *126*, 6508.

